Chemokine nitration prevents intratumoral infiltration of antigen-specific T cells

Barbara Molon,[1] Stefano Ugel,[1,2] Federica Del Pozzo,[3] Cristiana Soldani,[3] Serena Zilio,[4] Debora Avella,[3] Antonella De Palma,[5] PierLuigi Mauri,[5] Ana Monegal,[6] Maria Rescigno,[6] Benedetta Savino,[3] Piergiuseppe Colombo,[3] Nives Jonjic,[7] Sanja Pecanic,[7] Loretta Lazzarato,[8] Roberta Fruttero,[8] Alberto Gasco,[8] Vincenzo Bronte,[1] and Antonella Viola[3,9]

[1]Istituto Oncologico Veneto, Istituti di Ricovero e Cura a Carattere Scientifico (IRCCS) Venetian Oncological Institute, 35128 Padua, Italy
[2]Venetian Institute of Molecular Medicine, 35129 Padua, Italy
[3]Istituto Clinico Humanitas, IRCCS, 20089 Rozzano, Milan, Italy
[4]Department of Oncology and Surgical Sciences, University of Padua, 35128, Padua, Italy
[5]Institute for Biomedical Technologies (ITB-CNR), 20090 Segrate, Milan, Italy
[6]Department of Experimental Oncology, European Institute of Oncology, 20139 Milan, Italy
[7]Department of Pathology, Medical Faculty, University of Rijeka, 51000 Rijeka, Croatia
[8]Dipartimento di Scienza e Tecnologia del Farmaco, Università degli Studi di Torino, 10125 Torino, Italy
[9]Department of Translational Medicine, University of Milan, 20089 Rozzano, Milan, Italy

Tumor-promoted constraints negatively affect cytotoxic T lymphocyte (CTL) trafficking to the tumor core and, as a result, inhibit tumor killing. The production of reactive nitrogen species (RNS) within the tumor microenvironment has been reported in mouse and human cancers. We describe a novel RNS-dependent posttranslational modification of chemokines that has a profound impact on leukocyte recruitment to mouse and human tumors. Intratumoral RNS production induces CCL2 chemokine nitration and hinders T cell infiltration, resulting in the trapping of tumor-specific T cells in the stroma that surrounds cancer cells. Preconditioning of the tumor microenvironment with novel drugs that inhibit CCL2 modification facilitates CTL invasion of the tumor, suggesting that these drugs may be effective in cancer immunotherapy. Our results unveil an unexpected mechanism of tumor evasion and introduce new avenues for cancer immunotherapy.

CORRESPONDENCE
Barbara Molon:
barbara.molon@unipd.it

Abbreviations used: ACT, adoptive cell therapy; CHO, Chinese hamster ovary; MDSC, myeloid-derived suppressor cell; RNS, reactive nitrogen species; TIL, tumor-infiltrating lymphocyte; TRAMP, transgenic adenocarcinoma of the mouse prostate.

Adoptive cell therapy (ACT) for cancer, in which T cells are extracted from a cancer patient, expanded ex vivo, and readministered to the same patient, is increasingly the subject of clinical trials and has produced promising results, especially in cases where either surgery or chemotherapy failed to clear the tumor or its metastases (Gattinoni et al., 2006). The most remarkable results thus far have been produced in clinical trials of ACT for metastatic melanoma and the combination of surgery and ACT for hepatocellular carcinoma (June, 2007).

Current ACT protocols typically consist of isolating tumor-infiltrating lymphocytes (TILs) or peripheral CD8^{+} T cells from the patient before expanding the cells ex vivo, by either anti-CD3 mAb or peptide stimulation in the presence of IL-2, and then reinjecting them into the patient (Gattinoni et al., 2006). However, the efficacy of this approach is limited by several possible factors: lack of specificity of the transferred T cells, immune suppression of CD8^{+} T cell effector activity, and insufficient recruitment of the transferred T cells to the tumor site.

The ability of the transferred CD8^{+} cytotoxic T cells (CTLs) to recognize tumor antigens is an essential requirement for the efficacy of ACT. When peripheral CD8^{+} T cells are harvested from patients, their antigen specificity may be irrelevant to tumor recognition. A solution that has been proposed, and which is currently the focus of extensive research

efforts, is to modify the lymphocyte TCR via retroviral or lentiviral transduction of transgenic receptors, thus enabling cells to recognize the tumor-related antigens; alternatively, vaccinating the recipient with a tumor-specific antigen can enrich for T cells with the desired specificity (Gattinoni et al., 2006; Morgan et al., 2006; Johnson et al., 2009).

The local immunosuppressive effects of the tumor microenvironment are mediated by a variety of mechanisms, including expansion of regulatory T cells (T reg cells), tumor-associated macrophages, and myeloid–derived sup-pressor cells (MDSCs), as well as modification of arachidonic acid, L-tryptophan, or L-arginine metabolism (Colombo and Piconese, 2007; Viola and Bronte, 2007; Grohmann and Bronte, 2010). As a result of this suppressive activity, CTLs that are fully functional in vitro can be tolerized and thus lose their effector function at the tumor site. Nonetheless, com-bination therapies that link ACT with treatment targeting the mechanisms of local immunosuppression, such as lympho-depletion of the host by either irradiation or chemotherapy before cell transfer, promise to overcome this obstacle and are being actively pursued (Rosenberg and Dudley, 2009).

The combination of efforts to circumvent the two limiting factors described in the previous paragraphs has led to substan-tial progress, to the point that some of the solutions outlined in the previous paragraphs have reached the stage of clinical trials (Morgan et al., 2006; June, 2007; Johnson et al., 2009). How-ever, although there has been progress in ensuring that the transferred T cells in ACT are both capable of and undeterred from exerting their effector function and clearing the tumor, the efficiency of their recruitment to the main tumor and met-astatic sites has not received as much attention, although any clinical therapeutic regimen will be quantitatively dependent on the efficiency of such T cell recruitment. Indeed, one of the first in vivo studies of T cell trafficking in ACT suggested that, even accounting for the effects of immunosuppression, insuffi-cient T cell recruitment to the tumor site may be a critical fac-tor in the efficacy of therapy (Breart et al., 2008).

In this context, the first obvious problem is the anarchic vasculature of solid tumors, characterized by dilated and fragile vessels lacking hierarchical architecture. For example, cancer-induced overexpression of Rgs5 and the endothelin B receptor in pericytes and endothelial cells, respectively, in-hibits T cell homing into the tumor parenchyma (Buckanovich et al., 2008; Hamzah et al., 2008). However, even when capa-ble of reaching the tumor, T cells tend to remain at the pe-riphery, especially in the case of metastasis (Mukai et al., 1999; Galon et al., 2006; Boissonnas et al., 2007; Weishaupt et al., 2007), suggesting that other barriers inhibit the migration of CTLs to their cellular targets.

Protein nitration is the consequence of local production of reactive nitrogen species (RNS), such as the peroxynitrite anion (Szabó et al., 2007; Nathan and Ding, 2010). Several human cancers, including prostate, colon, liver (Kasic et al., 2011), breast, and ovarian (unpublished data) cancers, produce RNS, as indicated by their strong expression of nitrated tyro-sines (nitrotyrosine). In human prostate cancer, peroxynitrite
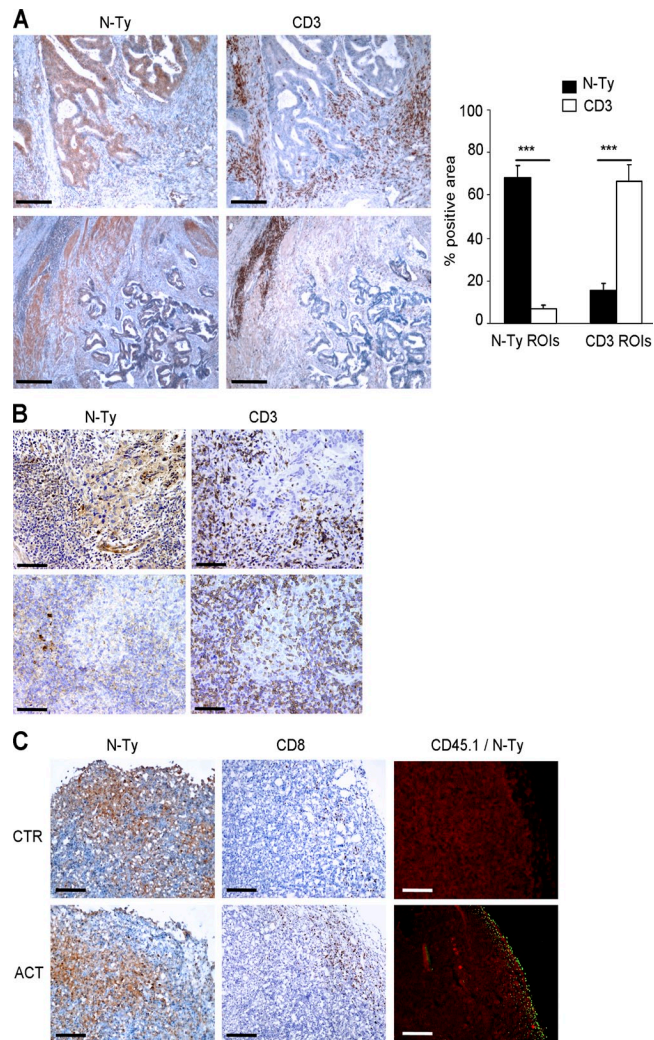
Figure 1. Chemical barriers inhibit T cell infiltration within the tumor. (A) Two representative serial sections of human colon carcinomas were immunostained (brown) for CD3 or nitrotyrosine, as indicated. Bars, 500 µm. Noncontiguous regions of interest (ROIs) with dimensions of 157 × 157 pixels were selected for either bright nitrotyrosine or CD3 staining and applied to serial sections. The percentages of immunoreactive areas for both nitrotyrosine and CD3 were obtained for each region of interest. ***, P < 0.001. Data are expressed as the means ± SE. (B) Two representative serial sections of human undifferentiated nasopharyngeal carcinomas were immunostained (brown) for CD3 or nitrotyrosine, as indicated. Bars, 200 µm. (C) CD45.1+ OT-I CTLs were adoptively transferred (ACT) to CD45.2+ mice bearing EG7-OVA tumors and, 4 d later, tumors were removed and stained to visualize nitrotyrosine-positive cells (N-Ty) and CTLs (either CD8+ or CD45.1+ cells). The first and second columns show the immunohistochemical detection of nitrotyrosine (N-Ty) and CD8+ T cells, respectively, whereas the third column shows immuno-fluorescence staining for CD45.1 (green) and N-Ty (red). Bars, 200 µm.

is generated by the interplay between the L-arginine metabo-lizing enzymes arginase (ARG) and nitric oxide synthase (NOS) and causes TIL unresponsiveness to stimuli, bypassing the TCR (Bronte et al., 2005). We have previously shown that drugs affecting ARG and NOS activity reduce intra-tumoral protein nitration and restore TIL function, suggesting

that intratumoral generation of RNS is one of the key mechanisms involved in tumor-induced immune dysfunctions (Bronte et al., 2005). Peroxynitrite is also produced by tumor-associated myeloid cells, including MDSCs (Bronte and Zanovello, 2005; Gabrilovich and Nagaraj, 2009). Nitration of the TCR complex by MDCS-derived RNS impairs tumor-specific immunity by reducing T lymphocyte responsiveness to tumor antigens (Nagaraj et al., 2007).

In this manuscript, we demonstrate that RNS exert additional immunosuppressive activities within the tumor microenvironment. Intratumoral RNS production results in posttranslational modification of the CCL2 chemokine and reduced access of TILs to the inner core of tumor tissues. In addition, we provide evidence that targeting RNS production in tumors can be exploited as a novel strategy to control immune evasion.

RESULTS

RNS can modify chemokines in the tumor microenvironment

Disease-free survival of patients with colorectal cancer strongly correlates with an increased ratio of T cells within the tumor relative to the tumor margins (Pagès et al., 2005; Galon et al., 2006). In tissues, protein nitration can be detected using an antibody that recognizes nitrotyrosine (Kasic et al., 2011), and by using this approach on human colorectal cancer tissue, we observed a singular pattern of T lymphocyte distribution that was the opposite of nitrotyrosine staining, with TILs concentrating at the border of the neoplastic lesions and cancer cells staining positive for nitrotyrosine (Fig. 1 A).

Among tumors that we have stained so far, undifferentiated nasopharyngeal carcinomas showed wide inter-tumor heterogeneity. In fact, in these cancers, we observed samples in which T lymphocytes were excluded from areas highly positive for nitrotyrosines and other specimens with a very marginal nitrotyrosine staining that were broadly infiltrated with T lymphocytes (Fig. 1 B). A similar pattern was observed in mice bearing an OVA-expressing tumor (EG7) after adoptive transfer of OVA-specific OT-I CTLs (Fig. 1 C), indicating that even bona fide tumor-specific effector CTLs are unable to reach the tumor core and are trapped at the cancer periphery.

Leukocyte migration into inflamed tissues, as in cancer, is driven by chemokines, small cytokines with selective chemoattractant properties (Viola and Luster, 2008). We hypothesized that, in addition to affecting T cell activation (Bronte et al., 2005; Nagaraj et al., 2007), RNS restrain TIL access to the tumor through posttranslational chemokine modifications.

CCL2 is produced by many cell types, including T cells, monocytes, and tumor cells, and it is a chemoattractant for myeloid cells, activated CD4+ and CD8+ T cells, and NK cells (Allavena et al., 1994; Carr et al., 1994). In addition, it is capable of triggering granule release from both NK and CD8+ T cells (Loetscher et al., 1996). Despite being one of the most frequently investigated chemokines in tumor immunology, the role of CCL2 in tumor immunity remains unclear, and several conflicting studies have been published (Rollins and Sunday, 1991; Bottazzi et al., 1992; Fridlender et al., 2010).
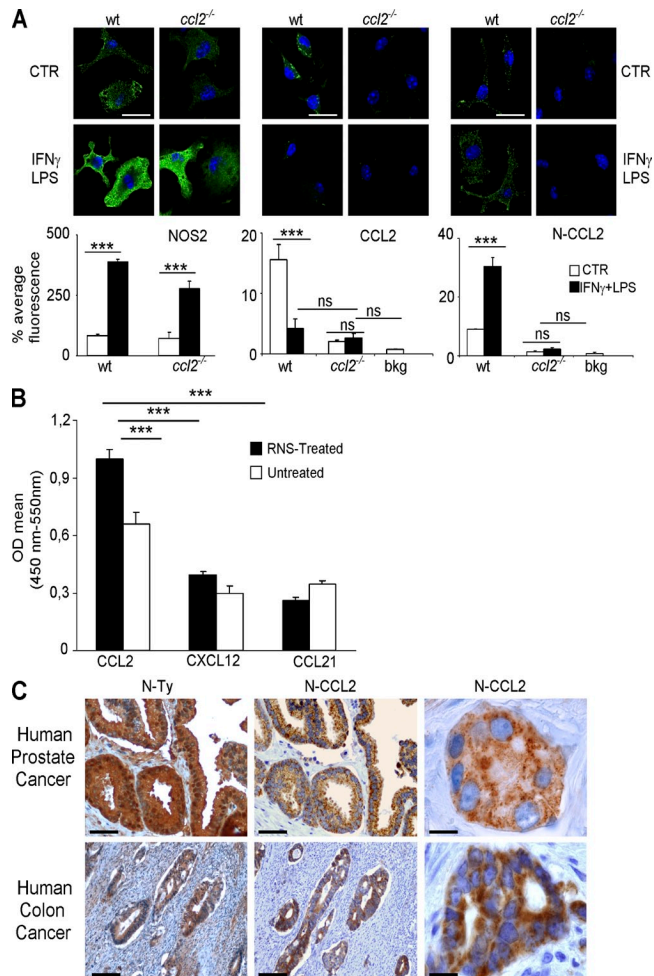
Figure 2. The RNS–modified CCL2 chemokine can be detected by specific antibodies. (A) Macrophages were cultured from the bone marrow of either wild-type (wt) or $ccl2^{-/-}/ccr2^{-/-}$ (indicated for simplicity as $ccl2^{-/-}$) mice. After stimulation with IFN-γ and LPS, macrophages were stained for NOS2, CCL2, or N-CCL2 (VHH-12BM). Background fluorescence with isotype-matched and secondary antibodies is reported in the graph and indicated as bkg. The graphs depict the mean fluorescence (mean ± SE, n = 10 ROIs). Statistical analysis was performed by a one-way ANOVA, followed by Tukey's test (***, P < 0.001). Bars, 20 µm. (B) VHH-12BM was tested in an ELISA against human CCL-2 and N-CCL2. Unmodified CCL2, CXCL12, CCL21, N-CXCL12, and N-CCL21 were used as negative controls. Data (A and B) are representative of at least three different experiments and are expressed as the means ± SE. ***, P ≤ 0.001. (C) Immunohistochemical staining of serial sections from human prostate (n = 12; top row) and colon (n = 12; bottom row) cancers. Cancer cells expressing N-CCL2 were present within the nitrotyrosine-positive area (bars, 200 µm). The last column shows a higher magnification of the same tissues (bars, 20 µm).

We verified that CCL2 was stably modified upon exposure to RNS. In addition, we included CXCL12 in our analysis because it belongs to a different chemokine family (CXC instead of CC). Chemokines were exposed to RNS (peroxynitrite) for 15 min, and the presence of reproducible modifications (i.e., nitration or nitrosylation) on single amino acids was determined by tandem mass spectrometry
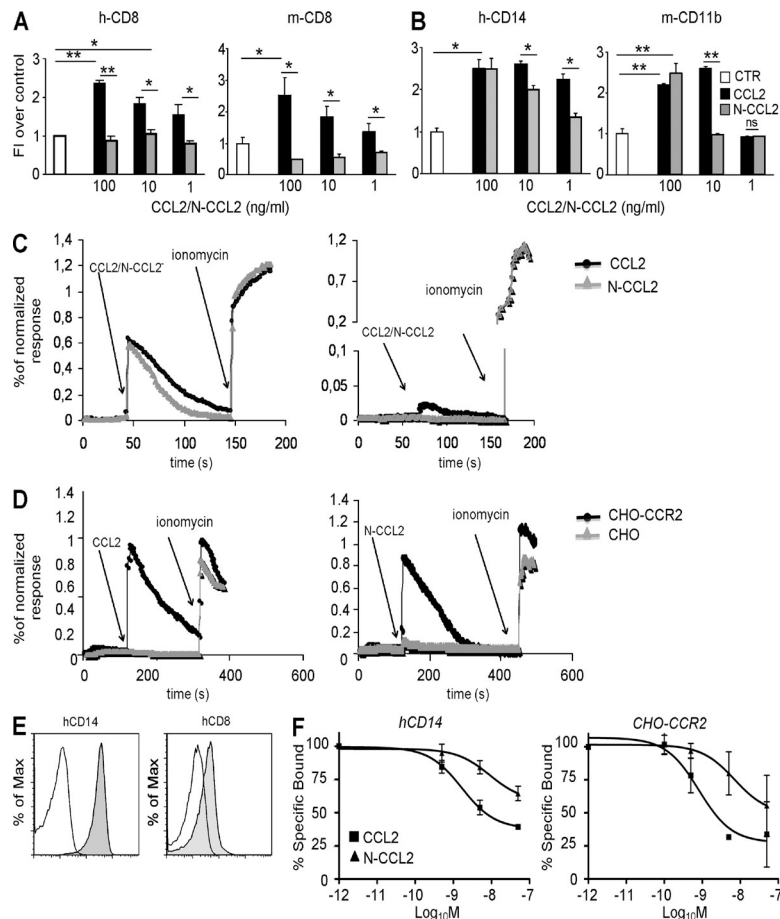
Figure 3. RNS alter the biological activity of human and mouse CCL2. (A and B) Human or mouse CD8^{+} T lymphocytes (A) and human CD14^{+} or mouse CD11b^{+} myeloid cells (B) were exposed to a gradient of recombinant human or mouse CCL2 (100, 10, or 1 ng/ml). Chemokines were either untreated (CCL2) or RNS treated (N-CCL2). Transmigrated cells were counted, and the results were expressed as fold induction over control. Data are representative of three different experiments and are expressed as the means ± SE. *, $P \leq 0.05$; **, $P \leq 0.01$. (C and D) Fluo-4/Fura-Red–loaded human T cells (CD14^{+} or CD8^{+}; A) or CHO cells that were or were not expressing human CCR2 (CHO or CHO-CCR2; D) were stimulated with either CCL2 or N-CCL2 and free $[Ca^{2+}]i$ was measured by flow cytometry. Ionomycin was used as a positive control for the maximal Ca^{2+} influx. Data are representative of one out of three experiments. (E) Human CD8^{+} and CD14^{+} cells were stained with either anti–human CCR2 phycoerythrin-conjugated mAb or with its isotypic control. Cell fluorescence was analyzed by flow cytometry. The mean fluorescence intensity, normalized to isotype control staining, was 13.2 ± 1.7 and 2.3 ± 0.3 for hCD14 and hCD8 cells, respectively ($P \leq 0.05$). (F) Competitive binding was performed by incubating CD14^{+} cells or CHO-CCR2 cells with ^{125}I-hCCL2 in the presence of various concentrations of unlabeled, untreated (■), or peroxynitrite-treated (Δ) hCCL2. After incubation, the cell-associated radioactivity was measured. Data are representative of three different experiments and are expressed as the means ± SE.

(MS-MS) coupled to liquid chromatography (LC-MS/MS). Tyrosine-nitrated KEWVQTY*IK and tryptophan-nitrated W*VQDSMDHLDK peptides were identified in mouse and human CCL2, respectively (where * represents nitration, +45 D; Fig. S1, A and B). Tyrosine-nitrated peptides from mouse CXCL12 (KPVSLSY*R and WIQEY*LEK; Fig. S1, C and D) were also characterized.

To verify the existence of RNS-modified chemokines in tumors, we tried to analyze tumor samples by LC-MS/MS, but chemokines were expressed in tumors at concentrations too low to be detected. Thus, we isolated a single-domain recombinant antibody (VHH) from a llama naive library (Monegal et al., 2009) that recognized the RNS-modified human and mouse CCL2 (N-CCL2). We tested this new reagent on bone marrow–derived macrophages that had or had not been exposed to a combination of IFN-γ and LPS to boost NOS2 expression and, thus, the nitration/nitrosylation of intracellular proteins (Kurata et al., 1996; Pfeiffer et al., 2001). N-CCL2 staining was stronger in stimulated macrophages than in resting ones, whereas CCL2 staining decreased in stimulated cells (Fig. 2 A), confirming our initial observations that RNS-modified CCL2 and CXCL12 are not recognized by commercially available anti-CCL2 or anti-CXCL12 antibodies, respectively (not depicted). In these experiments, $ccl2^{-/-}$ /$ccr2^{-/-}$ macrophages were used to verify the specificity of the N-CCL2
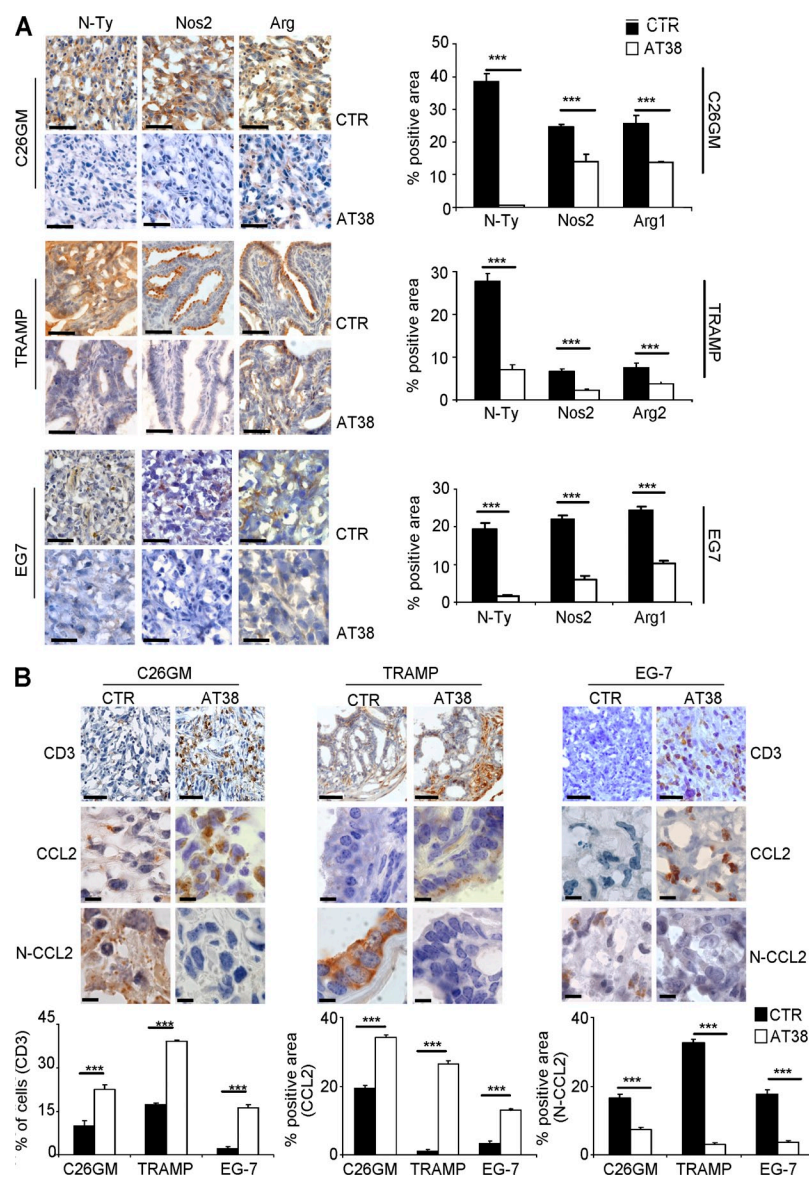
antibody (Fig. 2 A). ELISA results confirmed that the new antibody recognized N-CCL2 and not nonspecific modifications (nitration/nitrosylation) induced by RNS in chemokines (Fig. 2 B).

These results allowed us to evaluate the presence of N-CCL2 in human tissues. We obtained positive staining in specimens derived from human prostate and colon carcinomas (Fig. 2 C), two human cancers known to produce CCL2 (Hu et al., 2009; Izhak et al., 2010), indicating that N-CCL2 is expressed in both cancers. Most importantly, these data identified a novel posttranslational modification of chemokines that occurs in the human tumor microenvironment.

RNS–modified CCL2 attracts myeloid cells but not T lymphocytes

We analyzed the functional properties of N-CCL2. Short-term exposure of either the human or mouse chemokine to RNS had a strong impact on its ability to attract CD8^{+} T cells. Indeed, both human and mouse T cells were unable to migrate toward gradients of N-CCL2 in Transwell assays (Fig. 3 A). Similar results were obtained with CXCL12 (Fig. S2), indicating that RNS modification alters the biological properties of various chemokines.

In addition to CD8^{+} T cells, CCL2 attracts monocytes and macrophages to sites of inflammation (Serbina et al., 2008) and cancer (Sozzani et al., 1995). Moreover, the CCR2–CCL2 axis is crucial for the recruitment of MDSCs to tumors (Huang et al., 2007). Therefore, we analyzed the effects of RNS on the chemotactic activity of CCL2 toward myeloid cells.

Figure 4. Improved intratumoral T cell migration after in vivo reduction of RNS. (A and B) Immunohistochemical staining for nitrotyrosine, NOS2, ARG1, or ARG2 (A) or CD3, CCL2, and N-CCL2 (B) in C26GM, TRAMP, and EG7 tumor samples obtained from mice either treated or not with AT38 for 7 d. The graphs represent the quantification of immunoreactive cells or areas (Student's t test, ***, P < 0.001; n = 20). Bars: (A) 50 µm; (B, anti-CD3 pictures) 50 µm; (B, anti-CCL2 and anti-N-CCL2 pictures) 20 µm. Data are representative of three different experiments and are expressed as the means ± SE.

and T cells to the nitrated CCL2 were not dependent on the expression of different types of chemokine receptors. We next considered whether these opposite responses could be attributed to quantitative rather than qualitative differences. Indeed, we observed that CCR2 expression levels were much higher in myeloid cells than in CD8^{+} T cells (Fig. 3 E) and that RNS-induced modification resulted in an overall decreased affinity of CCL2 for its receptor but not in a complete loss of function (Fig. 3 F). Notably, because of the low CCR2 abundance in T cells, we failed to detect measurable binding of either CCL2 or N-CCL2 to lymphocytes (unpublished data). Altogether, these data suggest that the decreased affinity of N-CCL2 for CCR2 is functionally irrelevant for myeloid cells expressing many receptors, but decreased affinity impairs the capacity of T cells to sense the modified chemokine.

Our data indicate that RNS can induce stable posttranslational modifications in chemokines, which results in alteration of their functional properties. The RNS-induced modifications reduced the binding of CCL2 to CCR2 and the chemoattractant effect of CCL2 on CD8^{+} T cells. The fact that monocytes can be attracted by N-CCL2 might explain the selective enrichment of myeloid cells, compared with T lymphocytes, in the tumor microenvironment.

In vivo modulation of intratumoral RNS production results in enhanced TIL infiltration

We speculated that drugs that block intratumoral RNS production might interfere with factors that normally inhibit the access of T lymphocytes to the tumor mass. There is an ample list of compounds with in vitro peroxynitrite-scavenging activity but, for many of these molecules, the main activity is indirect and dependent on reactions with secondary radicals generated by peroxynitrite (Szabó et al., 2007). In any event, these compounds mainly act as extracellular traps, and we reasoned that molecules that affect RNS production by inhibiting the expression of enzymes involved in this process

The ability of CCL2 to attract either human or mouse myeloid cells was affected by RNS in a concentration-dependent manner (Fig. 3 B). Indeed, in contrast to what we observed with T lymphocytes, myeloid cells migrated efficiently in response to a high concentration (100 ng/ml) of RNS-modified CCL2, whereas their ability to sense lower concentrations of the RNS-modified chemokine (10–1 ng/ml) was reduced. In agreement with this result, we found that myeloid cells, but not T lymphocytes, responded to 100 ng/ml N-CCL2 with a rise in cytosolic calcium similar to that obtained upon stimulation with a control, unmodified chemokine (Fig. 3 C).

We next analyzed calcium responses elicited by either CCL2 or N-CCL2 in Chinese hamster ovary (CHO) cells that were or were not transfected with human CCR2. Transduction of human CCR2 was sufficient to assure a fully functional binding of both the control and modified chemokines (Fig. 3 D), suggesting that the different responses of myeloid

were better candidates for further development. Therefore, we designed, produced, and tested several new small molecules to block the in vivo generation of peroxynitrite and, among them, AT38 ([3-(aminocarbonyl)furoxan-4-yl]methyl salicylate; Suplemental data) possessed the highest activity and was thus selected for further in vivo studies.

We exploited three different tumor models to analyze the role of RNS in tumor immunity: a colon carcinoma (C26GM), a mouse thymoma engineered to express OVA as a tumor antigen (EG7-OVA), and a prostate cancer spontaneously arising in transgenic adenocarcinoma of the mouse prostate (TRAMP) mouse, which is considered a suitable model for evaluating results transferable to the clinical setting (Kaplan-Lefko et al., 2003). Mice injected s.c. with either C26GM or EG7-OVA cells and TRAMP mice (24 wk of age) were treated with AT38 for 7 d before tumor tissue collection. The intratumoral expression of nitrotyrosines and the enzymes NOS2 and ARG1, for C26GM and EG7-OVA tumors (De Santo et al., 2005), or NOS2 and ARG2, for TRAMP tissues (Bronte et al., 2005), decreased after in vivo administration of AT38 (Fig. 4 A).

Based on our hypothesis that RNS modification of chemokines might be responsible for the inability of T cells to reach the tumor core, we compared the T cell contents of tumors from mice that were or were not treated with AT38 and found that treatment had indeed significantly increased the number of T cells inside the tumors (Fig. 4 B). Notably, treating mice with AT38 induced a strong reduction in intratumoral N-CCL2 expression, which was paralleled by increased immunoreactivity for CCL2 (Fig. 4 B).

To prove that CCL2 nitration/nitrosylation was indeed responsible for defective TIL infiltration, we used two different experimental approaches. On the one hand, we performed the experiment shown in Fig. 4 in $ccr2^{-/-}$ mice and found that AT38 did not improve infiltration of $ccr2^{-/-}$ TILs in EG7-OVA tumors (Fig. 5 A). On the other hand, we injected unmodified CCL2 within the mass of untreated MCA-203 tumors and observed TIL recruitment into the tumor mass (Fig. 5 B). These data indicate that the mechanism by which AT38 improves TIL infiltration is based on unmodified chemokine (CCL2) bioavailability.

In vivo modulation of intratumoral RNS enhances tumor eradication by ACT

Altogether, the data described in the previous section suggest that AT38 administration in tumor-bearing mice could precondition the tumor microenvironment and thus support cancer elimination by adoptively transferred, tumor-specific CTLs. To verify this hypothesis, we initially used EG7-OVA tumor cells because specific antitumor CTLs can be obtained from OT-I transgenic mice; the CD8^{+} T cells isolated from these mice express a clonal TCR specific for the SIINFEKL peptide of OVA. Moreover, this tumor had been already used in previous lymphocyte trafficking studies (Boissonnas et al., 2007; Breart et al., 2008). As already described, treating mice bearing EG7-OVA tumors with AT38 caused an intratumoral
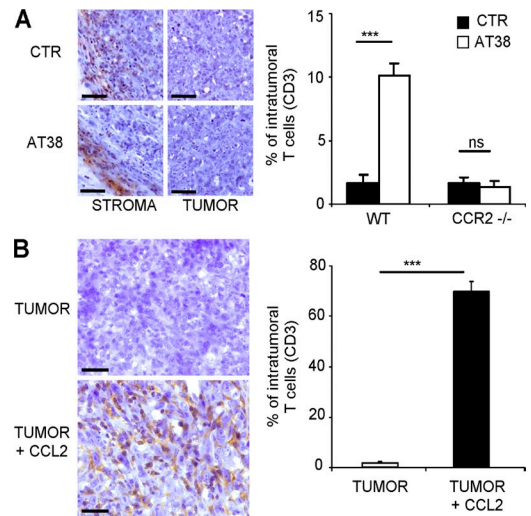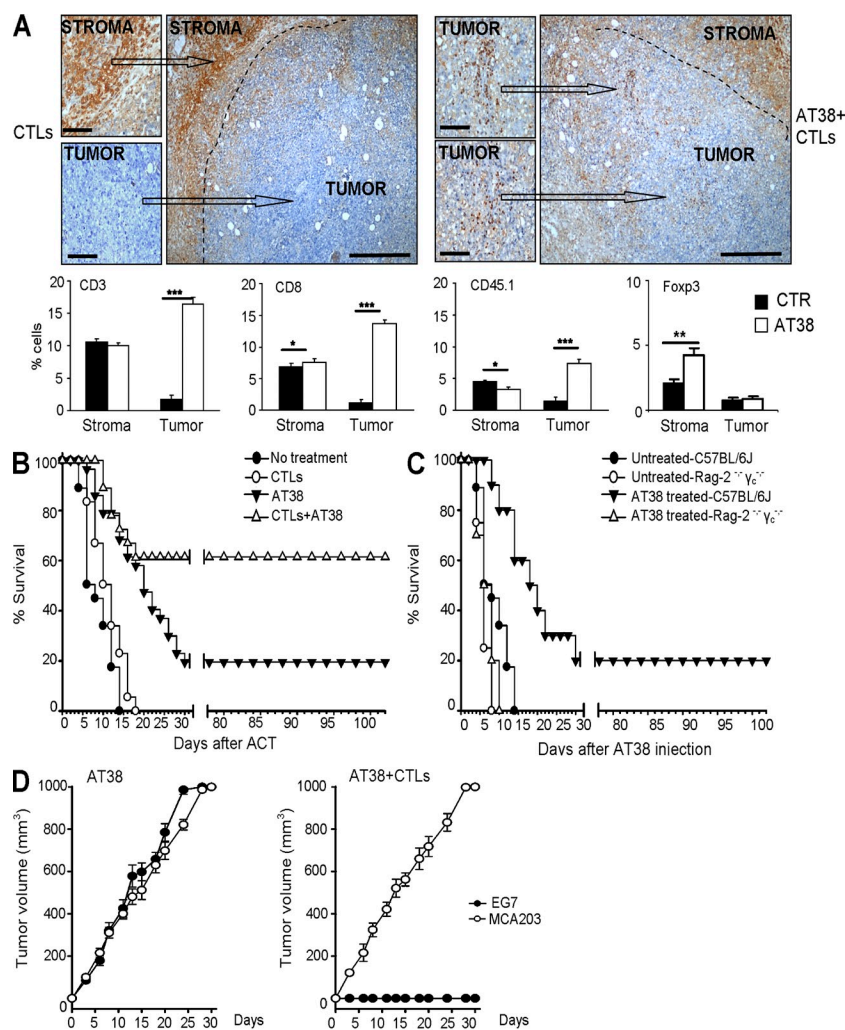

Figure 5.   CCL2 nitration/nitrosylation prevents intratumoral T cell infiltration. EG7 tumor samples obtained from either wt or $ccr2^{-/-}$ mice, treated or not with AT38 for 7 d (A) or MCA-203 tumor samples obtained from wt mice that had received intratumoral injections of CCL2 (0.5 µg in hydrogel; B) were stained for CD3 by immunohistochemistry. The graphs represent the quantification of immunoreactive cells (Student's t test; ***, $P < 0.001$; $n = 20$). Bars, 50 µm. Data are representative of three different experiments and are expressed as the means ± SE.

reduction in nitrotyrosines and N-CCL2, and it enhanced the expression of the unmodified chemokine (Fig. 4, A and B). The enhanced expression of CCL2 was not a result of increased protein synthesis in the tumor microenvironment (Fig. S3), reinforcing the concept that AT38 treatment unmasked CCL2 that, when otherwise modified by RNS, was not recognized by anti-CCL2 antibodies. Thus, we used AT38 to prepare the tumor microenvironment for the arrival of tumor-specific CTLs.

C57BL/6 (CD45.2) mice were injected s.c. with EG7-OVA cells and, when the tumor volume was ~150 mm³, the mice were or were not treated with AT38 for 4 d. This 4-d treatment did not modify the tumor volume (307 ± 52 vs. 332 ± 48 mm³ for untreated and AT38-treated mice, respectively). OVA$_{257-264}$-specific CTLs that had been obtained from OT-I mouse splenocytes (CD45.1) were then adoptively transferred into mice, and AT38 was further administered for an additional 3 d. AT38 administration allowed tumor invasion by antigen-specific CTLs that, as already discussed (Fig. 1 C), were otherwise trapped in the surrounding stroma (Fig. 6 A).

Inversion of the intratumoral ratio between CD8^{+} T lymphocytes and Foxp3^{+}/CD4^{+} T reg lymphocytes was correlated with the effect of immunotherapy on experimental melanoma (Quezada et al., 2006), and a high CD8^{+}/T reg cell ratio was found to be associated with a favorable prognosis in human epithelial ovarian cancer (Sato et al., 2005). We thus evaluated the presence of Foxp3^{+} cells in our experimental system. AT38 treatment did not alter the frequency of Foxp3^{+} cells within the tumor mass but, in contrast to what we had observed for antigen-specific CTLs, it caused a significant

Figure 6. Inhibition of RNS production promotes tumor infiltration and therapeutic effectiveness of adoptively transferred, tumor–specific CTLs. EG7-OVA tumor-bearing mice ($n = 18$) were either untreated or treated with AT38 for 7 d (30 mg/kg/d; AT38 only) with adoptive transfer of 2×10^6 CTLs (when the tumor volume was $\sim$300 mm^3; CTLs only) or with a combination of CTLs and AT38 (4 d before and 3 d after ACT; CTLs+AT38). (A) Mice were euthanized and tumors removed to analyze the frequency and localization of CD3$^+$, CD8$^+$, CD45.1$^+$, or Foxp3$^+$ T cells within the tumors. Immunohistochemical images are shown for CD3$^+$ T cells only, whereas the graphs represent the quantification of immunoreactive CD3$^+$, CD8$^+$, CD45.1$^+$, or Foxp3$^+$ T cells within the tumor and in the tumor-surrounding stroma. Data are expressed as the means $\pm$ SE. (Student's t test, *, P $\leq$ 0.05; **, P $\leq$ 0.01.***, P < 0.001; $n = 20$). Bars, 50 µm. (B) Tumors were measured blindly using digital calipers. Mice were euthanized when the tumor area reached 1,000 mm^3. Mantel-Haenszel statistics: CTLs versus AT38, P = 0.004; CTLs versus AT38+CTLs, P = 0.00003; AT38 versus AT38+CTLs, P = 0.029. (C) C57BL/6 ($n = 10$) and Rag2$^{-/-}$γc$^{-/-}$ ($n = 10$) mice were injected with 0.5×10^6 EG7-OVA cells. When the tumor volume reached $\sim$300 mm^3, the mice were treated or not with AT38 (30 mg/kg/d) for 7 d. Mantel-Haenszel statistics: C57BL/6J AT38-treated versus C57BL/6J, untreated, P = 0.0003; Rag2$^{-/-}$γc$^{-/-}$, AT38-treated versus Rag2$^{-/-}$γc$^{-/-}$, untreated, P = 0.352. (D) Mice that had been cured by either AT38 treatment ($n = 4$) or by the combined immunotherapeutic protocols (AT38 plus ACT, $n = 6$) were subcutaneously challenged after 100 d with the same EG7-OVA cells (0.5×10^6 cells/mouse), in one flank and an antigenically unrelated sarcoma (MCA-203, 10^6 cells/mice) that lacks OVA expression in the contralateral flank. The growth curve of the tumors is shown as an increase in the tumor volume over time from the day of the second tumor challenge. Data (A–D) are from two independent, cumulated experiments. In D, mean tumor volumes and S.E. are reported.

T reg cell accumulation at the boundary of the neoplastic lesion (Fig. 6 A). The CD8$^+$/T reg cell ratio was thus increased at the tumor core but decreased at the periphery.

We next asked whether the combination of AT38 and ACT might enhance the therapeutic effect. ACT alone in mice bearing 10-d-old ($\sim$300 mm^3) EG7-OVA tumors had no significant impact on tumor growth or mouse survival (Fig. 6 B and Fig. S4 A). Mice treated with AT38 alone had a modest but significant increase in survival, resulting in a cure rate of $\sim$20%. However, ACT preconditioned with AT38 produced a significant overall prolongation of survival and a cure rate of $\sim$60% of the tumor-bearing mice (Fig. 6 B and Fig. S4 A).
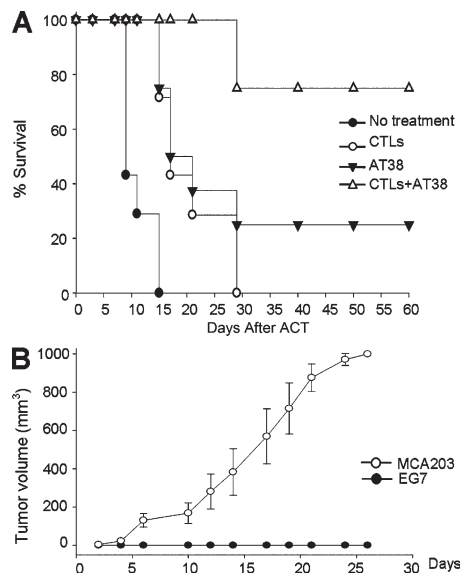
To understand whether the increased survival rate observed in the mice treated with AT38 only was the result of either a direct antitumor effect or the activation of endogenous immune responses, EG7-OVA cells were inoculated into either control or immunodeficient Rag2$^{-/-}$γc$^{-/-}$ mice that had been treated with AT38 according to the previous protocol. The results clearly showed that AT38 stimulates an endogenous antitumor response in immunocompetent mice, independent of ACT (Fig. 6 C and Fig. S4 B).

A major goal of all immunotherapeutic approaches is the establishment of long-term protection that will not only reduce the tumor burden but also eliminate all cancer cells. We therefore analyzed the establishment of antitumor memory responses in mice that had rejected the first tumor challenge. Mice that were cured by administration of AT38 or the combined immunotherapeutic protocols (AT38 plus ACT) were challenged subcutaneously after 100 d with the same EG7-OVA cells in one flank and an antigenically unrelated sarcoma (MCA-203) lacking OVA expression in the contralateral flank. Long-term survivors that had received AT38 plus ACT completely rejected the EG7-OVA but not the MCA-203 tumors, whereas mice surviving after administration of only AT38 did not reject any of the tumors, a clear indication that, although AT38 allowed an immune-mediated rejection of the first tumor, a memory response was generated only in mice that received ACT (Fig. 6 D). These results,

Figure 7. Inhibition of RNS production boosts ACT with mTERT-specific CTLs. (A) MCA-203 fibrosarcoma-bearing mice ($n = 8$) were either untreated or treated with AT38 for 7 d (AT38) with adoptive transfer of 2×10^6 CTLs specific for the mTERT antigen (when the tumor volume reached ~300 mm^3; CTLs) or with a combination of CTLs and AT38 (4 d before and 3 d after ACT; CTLs+AT38). Mantel-Haenszel statistics: CTLs versus AT38, P = 0.18; CTLs versus AT38+CTLs, P = 0.00009; AT38 versus AT38+CTLs, P = 0.018. (B) Mice that had been cured by the combined immunotherapeutic protocols (AT38 plus ACT, $n = 6$) were subcutaneously challenged after 60 d with the same MCA-203 cells (10^6 cells/mice) in one flank and an antigenically unrelated EG7-OVA (0.5×10^6 cells/mice) in the contralateral flank. The tumor growth curve is shown as an increase in the tumor volume over time from the day of the second tumor challenge. Data are from two independent, cumulated experiments. In B, mean tumor volumes and S.E. are reported.

together with those from the experiments in immunodeficient mice, suggest that NK cells, a short-memory adaptive immune response, or a combination of both are responsible for the effects of AT38 on tumor growth when administered alone in tumor-bearing mice.

To further corroborate the activity of AT38, we repeated the ACT experiments using CTLs that recognize the tumor antigen mouse telomerase (mTERT). Adoptive transfer of mTERT-specific CTLs in wild-type mice bearing 200-mm^3 subcutaneous nodules of MCA-203 fibrosarcoma had no effect on tumor regression, unless preceded by myeloid and lymphoid ablation (Marigo et al., 2010; Ugel et al., 2010). However, AT38 allowed mTERT-specific CTLs to reject the tumor even in the absence of lympho-myeloablation (Fig. 7 A). The surviving mice were challenged on day 60 with the same fibrosarcoma, which was promptly rejected (Fig. 7 B), indicating the presence of a persistent antitumor immunity.

DISCUSSION

Of the rate-limiting steps in effective active immunotherapy, recruitment and activation within the tumor milieu are now viewed as the most relevant. Several studies have shown that

T cells do not freely travel within a tumor; instead, they remain trapped in the stroma surrounding the cancer cells (Mukai et al., 1999; Galon et al., 2006; Boissonnas et al., 2007; Weishaupt et al., 2007). There are alterations in the endothelium of the tumor microvasculature (Weishaupt et al., 2007; Buckanovich et al., 2008; Hamzah et al., 2008) that are responsible for the reduced T cell extravasation and homing in the neoplastic lesion. Additionally, when the micropattern of T cell infiltration within the tumor is analyzed, other factors seem to be involved in the selective lack of direct contact between CTLs and tumor cells.

The homing of effector T cells to inflamed tissues and tumors depends on the concerted action of adhesion molecules, such as LFA-1 and VLA-4, and specific chemokines that regulate both leukocyte extravasation and migration toward specific areas (Springer, 1994; Butcher and Picker, 1996; Frederick and Clayman, 2001; Homey et al., 2002). Interestingly, in addition to inflammatory and endothelial cells, tumor cells themselves are capable of producing CTL-attracting chemokines (Murphy, 2001; Harlin et al., 2009). The role of chemokines in the tumor microenvironment is multifaceted in that chemokines can attract dendritic cells and lymphocytes, which may promote antitumor immunity and thus inhibit tumor growth; however, chemokines can also promote tumor growth and progression, angiogenesis, and metastasis (Balkwill and Mantovani, 2001). Thus, alterations in the expression or function of chemokines may have a tremendous impact on tumor development. Oncogenes might directly control the expression of chemokines that are crucial for T cell recruitment. For example, abnormalities in the EGFR–Ras signaling pathway in keratinocytes suppress the production of CCL27, and the consequent reduction in leukocyte recruitment could be partly responsible for tumor escape from the immune system (Pivarcsi et al., 2007).

However, the activity of chemokines is controlled not only through the regulation of their expression but also through silent decoy receptors and by posttranslational modifications, including proteolytic processing, glycosylation, deamination, or citrullination of the chemokines themselves (Loos et al., 2009). In this manuscript, we describe a novel mechanism of tumor escape based on the posttranslational modification of intratumoral chemokines, which can be pharmacologically targeted to improve the efficacy of immunotherapy. Our data indicate that CCL2, an inflammatory chemokine involved in the recruitment of CTLs and myeloid cells to tumors (Sozzani et al., 1995; Brown et al., 2007; Huang et al., 2007; Harlin et al., 2009), is nitrated/nitrosylated in human and mouse cancers. Interestingly, RNS-induced modifications change the functional properties of the chemokine so that it can no longer attract tumor-specific CTLs but can still recruit myeloid cells to the tumor. Although, for technical reasons, we could not overexpress CCR2 in CD8$^+$ T cells or reduce its expression in monocytes (electroporation dramatically downmodulates CCR2 expression), the reduction in CCL2 affinity for its receptor by nitration suggests that the differential responses of lymphocytes and monocytes to N-CCL2 may be

explained by the different CCR2 expression levels in the two cell populations.

Peroxynitrite reacts with several amino acids and directly modifies cysteine, methionine, and tryptophan, whereas tyrosine, phenylalanine, and histidine are modified through intermediary secondary species (Abello et al., 2009). Our in vitro experiments identified reproducible modifications on tyrosine and confirmed that nitration of tryptophan occurs. These findings support MS-MS as the gold standard for localizing nitrated amino acids. However, even if sensitivity of the MS instrumentation has increased (LOD < fmol level), it is not yet sufficient for detecting nitration in vivo (Abello et al., 2009).

ARG and NOS co-activation within the same environment can lead to production of several ROS and RNS. For example, superoxide (O_2^-) might be alternatively released from the NOS2 reductase domain at a low L-arginine environmental concentration as a result of enhanced ARG1 activity (Xia and Zweier, 1997; Xia et al., 1998; Bronte et al., 2003; Bronte and Zanovello, 2005), such as in the tumor microenvironment (Grohmann and Bronte, 2010). This phenomenon is known as the uncoupled reaction and, in addition to NOS2, NOS1 and NOS3 produce O_2^- in the presence of a low availability of L-arginine (Andrew and Mayer, 1999). Once generated, O_2^- reacts immediately with residual NO, leading to the formation of peroxynitrite (Nathan and Ding, 2010). Release of peroxynitrite from myeloid cells, activated by tumors and migrated to draining lymph nodes, might nitrate tyrosine residues in the TCR and CD8 receptors, resulting in decreased recognition of peptide–MHC complexes by the TCR (Nagaraj et al., 2007). It has been suggested that, in this context, peroxynitrite is generated in tumor-conditioned MDSCs by the combined activity of an NADPH oxidase (likely the Nox2 member of this family of oxidases) and an NOS isoform different from NOS2 (Nagaraj et al., 2007).

Nitroaspirin effect has been associated with a profound inhibition of both ARG1 and NOS2 activity in spleen and tumor-associated myeloid cells; although NO released by nitroaspirin was essential for NOS inhibition, as previously demonstrated (Griscavage et al., 1995; Mariotto et al., 1995), the aspirin-spacer portion was responsible for the ARG inhibition (De Santo et al., 2005). Moreover, nitroaspirin (but not aspirin) inhibits the catalytic subunit of NADPH oxidase and superoxide production induced by LPS, TNF, and IL–1α in pulmonary artery vascular smooth muscle and endothelial cells (Muzaffar et al., 2004). However, despite all of these positive activities, nitroaspirin was poorly effective as an adjuvant for ACT in the present work (unpublished data). For this reason, we designed novel drugs with different structural changes and alternative NO-donating groups. This process of screening culminated in the identification of AT38 as the lead compound (Supplemental data).

Our results indicate that in vivo administration of AT38 to tumor-bearing mice controls RNS generation and induces a massive T cell infiltration within the tumor microenvironment. On the basis of these data, we reasoned that AT38, by removing the chemical barriers raised by cancer growth,

could dramatically improve the efficacy of ACT protocols. Indeed, we found that AT38 enabled ACT to reject solid tumors, even at low T cell transfer doses, which are normally ineffective. Thus, RNS-inhibiting molecules represent a bona fide new class of adjuvants specific for the immunotherapy of cancer.

In a recent survey of intratumoral CTL trafficking by two-photon imaging, limited numbers of antigen-activated OT-I CD8^{+} T lymphocytes caused regression of OVA-expressing tumors by engaging in multiple, long-lasting interactions with tumor cells (Breart et al., 2008). We did not observe direct antitumor activity in our transferred antigen-activated OT-I CTLs, but the stages during which the tumors were treated were rather different in the two studies (the tumors were 10 d old and ~300 mm[3] in our study compared with 5 d old and ~20 mm[3] in the previous one). The results of the two studies might suggest that the ability to migrate within tumor tissues is progressively impaired with tumor growth, likely because of progressive accumulation of RNS-mediated modifications of target chemokines. The hypoxic microenvironment generated with tumor growth could play a key role in this process. Hypoxia is known to induce NOS2 up-regulation and peroxynitrite production under ischemic conditions, either with or without malignant transformation (Melillo et al., 1995; Suzuki et al., 2002). Recently, hypoxia-inducible factor 1α was shown to drive the program leading to ARG1 and NOS2 up-regulation in mouse tumor-associated macrophages (Corzo et al., 2010; Doedens et al., 2010). It is therefore possible that T cell motility is preserved at the margins of a small tumor, thus explaining the data obtained using intravital microscopy (Breart et al., 2008), but is severely impaired within an established, hypoxic cancer.

In similar work analyzing the infiltration of OVA-specific CTLs by in vivo imaging, it was noted that 10-d-old tumors could be cured with a large dose (10[7]) of purified naive OT-I-GFP cells (Boissonnas et al., 2007). At an early phase after ACT (3–4 d), OT-I CTLs remained at the periphery of the tumor, whereas at a later phase (5–6 d), OT-I CTLs began to infiltrate within the tumor, provided that neoplastic cells expressed the OVA tumor antigen (Boissonnas et al., 2007). Interestingly, OT-I-naive CD8^{+} T cells favored the infiltration by polyclonal CTLs activated with OVA antigen in vitro before co-transfer, suggesting that OT-I cells could induce a change in the tumor microenvironment and make it permissive for infiltration by other activated T cells. ACT with high numbers of CTLs possessing a high-avidity TCR for a tumor antigen is known to result in the eradication of large, established tumors through a mechanism that involves killing the stromal cells that cross-present the same tumor antigen (Zhang et al., 2008). In accordance, by titrating the number of OT-I CTLs, we established that a threefold increase in the number of cells inoculated into tumor-bearing mice, from 2×10^6 to 6×10^6, was sufficient to unveil an initial but significant effect of ACT on tumor progression (unpublished data). This therapeutic activity correlated with an increase in the number of cells producing CCL2 (unpublished data),

suggesting that the massive inflammation and chemokine production obtained through the transfer of a large number of CTLs can shift the balance of the tumor microenvironment from inhibition to activation of antitumor immune responses. However, it must be pointed out that, in a true clinical setting, many tumor antigens are self-antigens, and the T cell immune responses raised against these antigens are often of low affinity. These low-affinity CTLs can recognize peptide-pulsed target cells but often fail to recognize endogenous antigens on tumor cells, which are usually presented at much lower concentrations, as we recently showed for the melanoma antigen TRP-2 and the ubiquitous tumor antigen TERT (De Palma et al., 2004; Mennuni et al., 2008; Ugel et al., 2010). It is thus highly unlikely that tumor antigen–specific, low-avidity CTLs trigger the event leading to complete regression of the tumor (Mennuni et al., 2008; Ugel et al., 2010), unless a high number of CTLs are administered, as required by many clinical ACT protocols (Rosenberg et al., 2008). The data shown in this paper on the combination of AT38 and ACT with mTERT-specific CTLs (Fig. 7 A) suggest that the use of molecules that destroy the chemical barriers raised by the tumor and facilitate CTL infiltration may constitute a feasible strategy for improving the efficacy of cancer immunotherapy.

MATERIALS AND METHODS

Mice, cell isolation, and cell lines. C57BL/6 (H-2b) and BALB/c (H-2d) mice were purchased from Charles River. $Rag2^{-/-}\gamma_c^{-/-}$ mice (H-2b) were purchased form Taconic. TRAMP mice (H-2b) were a gift from N.M. Greenberg (Fred Hutchinson Cancer Research Center, Seattle, WA). OT-1-CD45.1 (H-2b) mice were obtained by crossbreeding C57BL/6-Tg(TcraTcrb)1100Mjb/J mice (The Jackson Laboratory) and C57BL/6-CD45.1 mice, a gift from M.C. Colombo (Istituto Tumori, Milan, Italy). The $ccl2^{-/-}ccr2^{-/-}$ mice (Noda et al., 2006) were a gift from E.S. Mocarski (Emory Vaccine Center, Atlanta, GA). The $ccr2^{-/-}$ mice were a gift from M. Locati (Humanitas Research Institute, Milan, Italy).

The C26GM cell line was derived from the C26 colon carcinoma (H-2d) line genetically modified to release GM-CSF (Bronte et al., 2003). The C26-GM cells used in this study produced GM-CSF at levels of 10–15 ng/ml from 10^6 cells in 48 h. The EG-7-OVA (H-2b) and MCA-203 fibrosarcoma (H-2b) cell lines were obtained from the American Type Culture Collection. These cell lines were grown in DME (Invitrogen) supplemented with 2 mM L-glutamine, 10 mM HEPES, 20 μM 2-mercaptoethanol, 150 U/ml streptomycin, 200 U/ml penicillin, and 10% heat-inactivated FBS (Invitrogen). MSC-2 cells were generated as previously described (Apolloni et al., 2000) and cultured in RPMI medium supplemented with 2 mM L-glutamine, 1 mM sodium pyruvate, 150 U/ml streptomycin, 200 U/ml penicillin, and 10% heat-inactivated FBS (Bichrom).

Human PB CD8+ T cells and CD14+ monocytes were sorted by negative selection using the RosetteSep kit (STEMCELL Technologies) and the Monocyte Isolation kit II (Miltenyi Biotec), respectively, on different healthy donors. Cells were cultured in RPMI 1640 medium (Invitrogen) supplemented with 10% FCS, 2 mM L-glutamine, 100 U/ml penicillin, and 100 mg/ml streptomycin.

Mouse CD11b+ cells were sorted from healthy mice by positive selection using CD11b+ microbeads (Miltenyi Biotec). CTLs recognizing β-gal obtained from a C57BL/6 mouse immunized with pcmv-β-gal by in vitro stimulation with the β-gal DAPIYTNV peptide and limiting dilution cloning were cultured in complete DME supplemented with 10% FBS and 20 U/ml human recombinant IL-2 (rh-IL-2; Chiron Corporation). CHO-CCR2 cells were cultured in DME-F12 medium (Invitrogen) supplemented

with 10% FCS, 1% penicillin, and 1% L-glutamine and cultured in the presence of 0.5 mg/ml G418.

Mouse OVA$_{257-264}$ CTLs derived from OT-I splenocytes were stimulated once with 1 μM specific OVA$_{257-264}$ (SIINFEKL) Kb-restricted peptide. Cultures were grown for 7 d in DME–10% fetal bovine serum containing 20 IU/ml of recombinant human IL-2 (Novartis) at 37°C in 5% CO$_2$. Mouse TERT$_{198-205}$ CTLs were obtained from a mixed leukocyte peptide culture set up with vaccinated TRAMP splenocytes in the presence of 0.1 μM mTERT$_{198-205}$ peptide (VGRNFTNL). Peptides were purchased from JPT Peptide Technologies. Protocols allowing the animal experiments have been approved by the local ethical committee and communicated to the relevant Italian authority (Ministero della Salute, Ufficio VI), in compliance of Italian Animal Welfare Law (Law n 116/1992; http://www.unipd.it/unipdWAR/page/unipd/organizzazione1/it_Book75_Page3).

Bone marrow–derived macrophages. Tibias and femurs from either BALB/c or CCL2$^{-/-}$CCR2$^{-/-}$ mice were removed using sterile technique, and the bone marrow was flushed. The red blood cells were lysed with ammonium chloride. To obtain macrophages, 10^6 cells were plated on glass coverslips into 6-well plates in medium supplemented with 40 ng/ml M-CSF and maintained at 37°C in a 5% CO$_2$–humidified atmosphere for 4 d. Macrophages were then cultured for an additional 6 h in the presence of 25 ng/ml IFN-γ (PeproTech) followed by a 48-h incubation with 1 μg/ml LPS (Sigma Aldrich).

Tumor challenge. BALB/c mice were inoculated s.c. on the right flank with 0.5×10^6 C26GM cells. C57BL/6 and $Rag2^{-/-}\gamma_c^{-/-}$ mice were inoculated s.c with 0.5×10^6 EG7-OVA cells. C57BL/6 mice were inoculated s.c with 10^6 MCA-203 cells.

CTL assay. To generate in vitro CTLs, 6×10^5 splenocytes from BALB/c mice were incubated with 6×10^5 γ-irradiated C57BL/6 splenocytes. After 5 d, the cultures were tested for their ability to lyse an allogeneic target in a 5-h ^{51}Cr-release assay. The percentage of specific lysis was calculated from the triplicate sample as follows: (experimental cpm − spontaneous cpm)/(maximal cpm − spontaneous cpm) × 100. Lytic units (LU) were calculated as the number of cells producing 30% specific lysis of 2,000 target cells/10^6 effector cells (L.U.$_{30}$/10^6 cells). When present, the nonspecific lysis of control targets was subtracted.

Proliferation assay. BALB/c splenocytes (7.5×10^5 cells/well) were cultured in 96-well flat-bottom plates (Falcon; BD) and stimulated with 1 μg/ml of plate-coated anti-CD3 and 5 μg/ml soluble anti-CD28 mAbs. The drugs were used at concentrations that lacked toxicity in a control culture (the concentration range was 3–200 μM). After 3 d of incubation, the cultures were pulsed with 1 μCi/well ^{3}HTdR (PerkinElmer) for 18 h, and ^{3}HTdR incorporation was measured by scintillation counting. Data are expressed as cpm (means ± SD) of triplicate cultures.

Adoptive cell transfer (ACT). The effects of ACT in mouse transplantable tumor models were investigated in C57BL/6 and $Rag2^{-/-}\gamma_c^{-/-}$ mice after an s.c. challenge with 5×10^5 EG7-OVA cells. When the tumor area reached ∼300 mm³, the mice were treated with either 30 mg/kg/d of AT38 in 1% carboxymethyl cellulose/ethanol (vehicle) or vehicle alone through a double i.p. injection. This treatment was repeated every day for 4 d. After that, the mice were treated with 2×10^6 of antigen-activated OVA$_{257-264}$ CTLs through i.v. injection. At the time of the CTL transfer, the mice were injected with 30,000 IU of recombinant human IL-2, administered twice a day i.p for 3 consecutive days. A group of mice was also treated with AT38 for 3 d after ATC. The tumors were measured on blind using digital calipers. The mice were euthanized when tumor area reached 1,000 mm³.

Hydrogel preparation and injection. Biodegradable, injectable, and photo-cross-linkable hydrogel was prepared as previously described (Rossi et al., 2011). C57BL/6 mice were inoculated s.c with 10^6 MCA-203 cells. 40 mg/liter of the polymeric hydrogel solution was photoactivated using a

366-nm light source for 30 s (BlueWave 50 lamp; Dymax). Preactivated polymeric solution was injected through a Hamilton syringe (GA 22s/51 mm/PST2) for in situ cross-linking and hydrogel formation. Hydrogel containing 0.5 µg mCCL2 (R&D Systems) or not was inoculated within the tumor. The day after the inoculation, the tumors were explanted, fixed in PLP fixative (paraformaldehyde/lysine/periodate), cryoprotected in 30% sucrose, and frozen in OCT. Tumor samples were cut with a cryostat (6 µm), fixed with acetone for 3 min, and stained with an anti–CD3 polyclonal antibody (1:50; Dako). The appropriate secondary antibody was used.

Chemokine nitration/nitrosylation. Recombinant human and mouse CXCL12 and CCL2 were purchased from R&D Systems. Chemokine nitration/nitrosylation was performed by mixing the recombinant protein (CXCL12 or CCL2) with 1 mM peroxynitrite (Millipore) at 37°C for 15 min in a final volume of 100 µl PBS containing 0.1% BSA (Sigma-Aldrich). After incubation, the samples were dialyzed overnight using the Slide-A-Lyzer Dialysis cassette kit, 3,500 MWCO (Thermo Fisher Scientific), preparing 2 liter PBS containing 0.1% BSA according to the kit's instructions. The next day, chemokines were collected from the dialysis cassettes and used for assays.

Chemotaxis assay. Human T cells (CD3$^+$ and CD8$^+$), human CD14$^+$ cells, mouse CD11b$^+$ cells, or mouse CD8$^+$ T cells were collected and washed three times in basal medium (serum-free medium containing 0.1% BSA). The cells were seeded in the upper chamber of a 3-µm pore size Transwell plate (Corning) in basal medium. The lower chambers were filled with basal medium alone or basal medium containing untreated or RNS-modified dialyzed chemokine (CXCL12, 50 ng/ml; CCL2, 20 or 100 ng/ml). After 3 h at 37°C, the number of cells that had migrated into the lower chamber was estimated by flow cytometry on a FACSCalibur system (BD).

Binding assays. CCL2 competitive binding was performed by incubating 3×10^5 CHO-K1 cells stably transfected with human CCR2 or 2.5×10^5 human monocytes with 100 pM ^{125}I-CCL2 in the presence of different concentrations of unlabeled CCL2, N-CCL2, or CXCL8 in binding buffer (DME-F12, 4 mM Hepes, pH 7.4, and 1% BSA) at 4°C for 2 h. After incubation, the cell-associated radioactivity was measured. To estimate the Kd (equilibrium dissociation constant) of CCL2, the homologous competitive binding and N-CCL2 inhibition curves were determined by nonlinear regression using a one-site competitive binding equation in Prism software (3.0a; GraphPad Software).

Calcium measurements. Human CD8$^+$ or CD14$^+$ cells or CHO-K1/CCR2 cells were loaded with 4 µg/ml Fluo-4 AM and 10 µg/ml Fura Red AM for 30 min at 37°C in 1% FCS-RPMI 1640 medium. Cells were washed once and resuspended in 1% FCS HBSS medium. After washing, the cells were kept at room temperature (25°C) in the dark. A 500-ml aliquot was warmed to 37°C before fluxing. First, a baseline (120 s) level was recorded. Then, the tube was removed, 100 ng/ml hCCL2 was added and the tube was replaced. The experiment was recorded for an additional 120 s. We applied ionomycin stimulation (1 µg/ml) as a positive control to verify equal dye loading.

The Ca^{2+} ratio (Fluo-4/Fura-Red) was measured over time using a FACSCanto (BD) and analyzed with FlowJo software. The results are expressed as percentages of normalized response, calculated as follows: ([median of Fluo-4/Fura-Red ratio] − [mean of the medians of Fluo-4/Fura-Red ratio before CCL2 addition])/([mean of the medians of Fluo-4/Fura-Red ratio during the response to ionomycin] − [mean of the medians of Fluo-4/Fura-Red ratio before CCL2 addition]).

Enzymatic digestions. Human CXCL12, human CCL2, or mouse CCL2, untreated or RNS modified, were digested with trypsin (sequencing grade modified from Promega). Trypsin was added to the chemokines at an enzyme-to-substrate ratio of 1:50 (vol/vol) in 100 mM ammonium bicarbonate, pH 8.0, and incubated overnight at 37°C. The reaction was stopped by adjusting the pH to 2.0 with the addition of TFA. Peptide samples were purified and concentrated using PepClean C-18 (Thermo Fisher Scientific),

according to the manufacturer's instructions. A 10-µl aliquot of the peptide mixture was applied to LC-MS/MS.

MS analysis. One-dimensional LC-MS analyses of the tryptic digest were performed with a modified configuration of the ProteomeX 2D LC-MS workstation (Thermo Fisher Scientific). A 10-µl aliquot was directly loaded on a reversed-phase column (Biobasic-18, 0.180 i.d. × 100 mm, 5 µm, 300 ′Å; Thermo Fisher Scientific) and separated with an acetonitrile gradient (eluent A, 0.1% formic acid in water; eluent B, 0.1% formic acid in acetonitrile); the gradient profile was 5% eluent B for 1 min followed by 5–65% eluent B gradient within 30 min. The peptides eluted from the C18 column were directly analyzed with a linear ion trap LTQ mass spectrometer equipped with nanospray (Thermo Fisher Scientific). The main MS conditions were the following: heated capillary at 185°C, ion spray at 3.0 kV, and capillary voltage at 38 V. Spectra were acquired in the positive mode (in the range of 400–2,000 m/z) using data-dependent scan and dynamic exclusion modes for MS/MS analysis (collision energy 35%, three most abundant ions, minimum count 3).

Isolation of VHHs against N-CCL2. Recombinant VHHs against RNS-modified CCL2 were isolated from a llama single-domain naive library (Monegal et al., 2009) after three rounds of panning. In all three rounds, phages were predepleted against nonmodified CCL2 and the peroxynitrite reaction crude before exposing them to N-CCL2.

The following were coated on a MaxiSorp 96-well plate: 1 µg of nonmodified CCL2 and 1 mM peroxynitrite reaction crude (for depletion) or 1 µg human N-CCL2. The wells were blocked with 3% BSA in PBS 0.1% Tween at room temperature for 2 h and washed three times with PBS before the addition of naive library phages. In the first round, 3×10^{15} phages were depleted against CCL2 and the peroxynitrite crude before using them for panning against the RNS-modified CCL2. After a 2-h incubation at room temperature, the wells were washed 10× with PBS 0.1% Tween and 10× with PBS, and bound phages were eluted with 0.1 M triethylamine, pH 11.0. The eluted phages were titrated, used to infect TG1 cells, and plated on 2xTY ampicillin, glucose large square plates. Colonies were scraped, infected with 10^{10} KM13 helper phage, and grown overnight, and phage particles were precipitated from the culture supernatant with 4% PEG 6000 and 0.5 M NaCl. The new sublibrary of phages was resuspended in sterile PBS, titrated, depleted against CCL2 and peroxinytrite, and used in the second round of panning. The same complete procedure was repeated for the third round, with the following modifications: panning alternating 3% BSA in PBST and 2% skim milk in PBS were alternated as blocking agents, and 0.5 µg of RNS-modified CCL2 was used instead of 1 µg. In each round of panning, the enrichment of the phage sublibrary obtained was calculated as the ratio of output/input phage. A total of 96 single clones were analyzed by ELISA after the third round of panning. Colonies were grown at 37°C in 2xTY supplemented with 0.1 mg/ml ampicillin and 0.1% glucose for 3–4 h, induced with 1 mM IPTG and incubated overnight at 30°C. Cultures were harvested and periplasmic lysates containing soluble HA-tagged VHHs were diluted 1:3 and incubated with 10 µg/ml mouse supernatant anti-HA 12CA5 for use in ELISA. MaxiSorp 96-well plates (Nunc) were coated with either N-CCL2 or CCL2 or with crude reaction (peroxynitrite) in 50 mM sodium carbonate buffer as a negative control (4°C). Antigens were used at the same concentrations as for panning. The plates were blocked with 2% BSA for 2 h, washed three times with PBS, and incubated 1 h with periplasmic lysates. The plates were then washed three times with PBS-0.1% Tween and treated with anti–mouse HRP conjugate (Bio-Rad Laboratories) for 1 h at room temperature. After washing three times with PBST, the reaction was developed by adding TMB (Thermo Fisher Scientific), and the absorbance at 450 nm was measured after a 20-min incubation. Clones that had an absorbance value in the N-CCL2 coated plate that was significantly different from the value of both CCL2 or the crude reaction-coated plate were used for immunohistochemical analysis.

Quantitative (q) RT-PCR. Total RNA was isolated from the tumor tissue of EG7-OVA tumor-bearing mice that were or were not treated with 30 mg/kg/d of AT38 using the RNAspin Mini RNA Isolation kit

(GE Healthcare) according to the manufacturer's instructions. RNA was reverse transcribed using the High-Capacity cDNA Reverse Transcription kit (Applied Biosystems). Quantitative PCR analysis was performed with the TaqMan Gene Expression MasterMix (Applied Biosystems). The following probes were used: for Actin TaqMan Gene Expression Assay, Mm00607939_s1 (Applied Biosystems), and for CCL2 TaqMan Gene Expression Assay, Mm00203002_m1 (Applied Biosystems). qRT-PCR data were expressed as the CCL2 expression level (normalized AU) of three tumor samples.

Immunohistochemistry and immunofluorescence. Mouse tumors were fixed in PLP fixative (paraformaldehyde/lysine/periodate), cryoprotected in 30% sucrose and frozen in OCT. The samples were cut with a cryostat (6 µm) and fixed with acetone for 3 min. The primary antibodies used were the following: anti-nitrotyrosine (1:400; Millipore), anti-CD3 (1:50; Dako), anti-CD8 (1:20; eBioscience), anti-CD45.1 (1:100; BioLegend), anti-NOS2 (1:200; Neo-Markers), anti-ARG1 and anti-ARG2 (1:50; Santa Cruz Biotechnology, Inc.), anti-CCL2 (1:10; R&D Systems), anti-Foxp3 (1:50; eBioscience), and anti–N-CCL2 (VHH-12BM). The appropriate secondary antibodies were used.

For human tumor samples, this study was conducted in accordance with the guidelines of the Ethics Committee of the hospital treating the patients (Istituto Clinico Humanitas, Rozzano, Milan, Italy). Paraffin-embedded tissues from 12 colonic adenocarcinomas and 12 prostate cancers were retrieved from the archives of the hospital's Department of Pathology. One slide from each specimen was stained with hematoxylin and eosin, and all histological features were reviewed by our pathologist to confirm the diagnosis. Cases with necrosis were excluded.

The tissues were serial cut with a microtome (2 µm) and deparaffinized, and the antigen retrieval was performed in a pressure cooker (Biocare Medical) using DIVA buffer (Biocare Medical). Endogenous peroxidase activity and nonspecific binding sites were blocked. The primary antibodies used were the following: anti-nitrotyrosine (1:400; Millipore), anti-CD3 (Dako), and anti-N-CCL2 (VHH-12BM). The appropriate secondary antibodies were used.

Immunoreactivity was visualized with 3,3-diaminobenzidine (DAB; Sigma-Aldrich). Sections were counterstained with hematoxylin and mounted in Eukitt. Immunofluorescence on frozen tissues was performed using anti-CD45.1 and anti-nitrotyrosine antibodies (see beginning of section); the appropriate secondary antibodies conjugated to Alexa Fluor 488 or Alexa Fluor 594 (Invitrogen) were used. The slides were mounted with ProLong (Invitrogen).

For in vitro NOS2 detection, C26GM cells, treated or not with 50 µM AT38 for 24 and 48 h, were fixed with 4% paraformaldehyde, permeabilized, and incubated with anti-NOS2 (1:200, NeoMarkers). The appropriate secondary antibodies were used. Nuclei were counterstained with 1 µg/ml Hoechst 33258 and mounted with ProLong (Invitrogen).

For each specimen, CD3^{+}, CD8^{+}, CD45.1^{+}, and Foxp3^{+} cells were counted by two different operators in 20 randomly selected fields of each slide at high magnification (400×). The expression of nitrotyrosines, NOS2, ARG1, ARG2, CCL2, and N-CCL2 in the sections was analyzed by automated data collection using a computer-assisted system (CellF; Olympus). The percentage of the area that was immunoreactive-positive was calculated for 20 randomly selected fields of each slide at high magnification (400×).

Mouse macrophages were fixed with 4% formaldehyde, permeabilized, and incubated with anti-NOS2 (1:200, NeoMarkers), anti-CCL2 (1:10; R&D Systems), or anti–N-CCL2 (VHH-12BM). The appropriate secondary antibodies were used.

Images were acquired with a microscope (BX51; Olympus) equipped with a Colorview IIIu digital camera (Olympus). Confocal microscopy was performed with a FluoView FV1000 (Olympus) using laser excitation at 405 and 488 nm. Images were acquired with an oil immersion objective (60× 1.4 NA Plan-Apochromat; Olympus). The images were processed using Photoshop (7.0; Adobe).

For quantitative analysis of the inverse correlation between the expression of nitrotyrosines and T cell infiltration in colon cancer, serial sections of different human colon carcinomas were analyzed by automated data collection using a computer-assisted system (CellF; Olympus). Different and noncontiguous regions of interest (ROIs) of 157 × 157 pixels were randomly selected, and their immunoreactive areas for nitrotyrosines or CD3 were quantified.

Western blotting. MSC-2 cells were cultured for 4 d in the presence of either 100 ng/ml IL-4 or 25 ng/ml IFN-γ. The cells were then treated or not with 25 or 50 µM AT38 for 24 and 48 h. Whole-cell extracts were obtained from 2×10^5 cells. The cells were collected and rinsed once in PBS, and then immediately frozen in liquid nitrogen. The samples were dissolved in 15 µl Laemmli buffer and denatured for 10 min at 98°C. The samples were separated electrophoretically on a 12% SDS-PAGE gel and transferred onto an Immobilon P membrane (Millipore). The immunoblots were probed with anti-ARG1 (Santa Cruz Biotechnology, Inc.) or anti-NOS2 (Santa Cruz Biotechnology, Inc.) Abs. Secondary HRP-conjugated Abs were obtained from GE Healthcare. The immunoblots were analyzed by ECL (GE Healthcare).

Statistical analysis. Statistical analyses were performed using the following: Student's unpaired two-tailed t test and ANOVA one-way test analysis with Tukey's Multiple Comparisons Test. Data are representative of at least three different experiments. Values are expressed as the means ± SE. Kaplan-Maier plots and the Mantel-Haenszel test were used to compare the survival of mice, and all pairwise multiple comparisons were analyzed with the Holm-Sidak method. The overall significance level was set at 0.05.

Online supplemental material. Fig. S1 shows the fragmentation (MS/MS) spectra of nitrated and control peptides from mouse CCL2, human CCL2, and mouse CXCL12. Fig. S2 shows that N-CXCL12 is not chemotactic for human and mouse T cells. Fig. S3 shows qRT-PCR results from tumor tissue extracts, indicating that AT38 treatment does not induce de novo CCL2 synthesis. In Fig. S4, tumor growth curves of single mice treated with a combination of AT38 and OVA$_{257-264}$–specific CTLs are shown. The Supplemental data describes the rationale behind the design and synthesis of AT38. Online supplemental material is available at http://www.jem.org/cgi/content/full/jem.20101956/DC1.

REFERENCES

Abello, N., H.A. Kerstjens, D.S. Postma, and R. Bischoff. 2009. Protein tyrosine nitration: selectivity, physicochemical and biological consequences, denitration, and proteomics methods for the identification of tyrosine-nitrated proteins. *J. Proteome Res.* 8:3222–3238. http://dx.doi.org/10.1021/pr900039c

Allavena, P., G. Bianchi, D. Zhou, J. van Damme, P. Jílek, S. Sozzani, and A. Mantovani. 1994. Induction of natural killer cell migration by monocyte chemotactic protein-1, -2 and -3. *Eur. J. Immunol.* 24:3233–3236. http://dx.doi.org/10.1002/eji.1830241249

Andrew, P.J., and B. Mayer. 1999. Enzymatic function of nitric oxide synthases. *Cardiovasc. Res.* 43:521–531. http://dx.doi.org/10.1016/S0008-6363(99)00115-7

Apolloni, E., V. Bronte, A. Mazzoni, P. Serafini, A. Cabrelle, D.M. Segal, H.A. Young, and P. Zanovello. 2000. Immortalized myeloid suppressor

cells trigger apoptosis in antigen-activated T lymphocytes. *J. Immunol.* 165:6723–6730.

Balkwill, F., and A. Mantovani. 2001. Inflammation and cancer: back to Virchow? *Lancet.* 357:539–545. http://dx.doi.org/10.1016/S0140-6736(00)04046-0

Boissonnas, A., L. Fetler, I.S. Zeelenberg, S. Hugues, and S. Amigorena. 2007. In vivo imaging of cytotoxic T cell infiltration and elimination of a solid tumor. *J. Exp. Med.* 204:345–356. http://dx.doi.org/10.1084/jem.20061890

Bottazzi, B., S. Walter, D. Govoni, F. Colotta, and A. Mantovani. 1992. Monocyte chemotactic cytokine gene transfer modulates macrophage infiltration, growth, and susceptibility to IL-2 therapy of a murine melanoma. *J. Immunol.* 148:1280–1285.

Breart, B., F. Lemaître, S. Celli, and P. Bousso. 2008. Two-photon imaging of intratumoral CD8+ T cell cytotoxic activity during adoptive T cell therapy in mice. *J. Clin. Invest.* 118:1390–1397. http://dx.doi.org/10.1172/JCI34388

Bronte, V., and P. Zanovello. 2005. Regulation of immune responses by L-arginine metabolism. *Nat. Rev. Immunol.* 5:641–654. http://dx.doi.org/10.1038/nri1668

Bronte, V., P. Serafini, C. De Santo, I. Marigo, V. Tosello, A. Mazzoni, D.M. Segal, C. Staib, M. Lowel, G. Sutter, et al. 2003. IL-4-induced arginase 1 suppresses alloreactive T cells in tumor-bearing mice. *J. Immunol.* 170:270–278.

Bronte, V., T. Kasic, G. Gri, K. Gallana, G. Borsellino, I. Marigo, L. Battistini, M. Iafrate, T. Prayer-Galetti, F. Pagano, and A. Viola. 2005. Boosting antitumor responses of T lymphocytes infiltrating human prostate cancers. *J. Exp. Med.* 201:1257–1268. http://dx.doi.org/10.1084/jem.20042028

Brown, C.E., R.P. Vishwanath, B. Aguilar, R. Starr, J. Najbauer, K.S. Aboody, and M.C. Jensen. 2007. Tumor-derived chemokine MCP-1/CCL2 is sufficient for mediating tumor tropism of adoptively transferred T cells. *J. Immunol.* 179:3332–3341.

Buckanovich, R.J., A. Facciabene, S. Kim, F. Benencia, D. Sasaroli, K. Balint, D. Katsaros, A. O'Brien-Jenkins, P.A. Gimotty, and G. Coukos. 2008. Endothelin B receptor mediates the endothelial barrier to T cell homing to tumors and disables immune therapy. *Nat. Med.* 14:28–36. http://dx.doi.org/10.1038/nm1699

Butcher, E.C., and L.J. Picker. 1996. Lymphocyte homing and homeostasis. *Science.* 272:60–66. http://dx.doi.org/10.1126/science.272.5258.60

Carr, M.W., S.J. Roth, E. Luther, S.S. Rose, and T.A. Springer. 1994. Monocyte chemoattractant protein 1 acts as a T-lymphocyte chemoattractant. *Proc. Natl. Acad. Sci. USA.* 91:3652–3656. http://dx.doi.org/10.1073/pnas.91.9.3652

Colombo, M.P., and S. Piconese. 2007. Regulatory-T-cell inhibition versus depletion: the right choice in cancer immunotherapy. *Nat. Rev. Cancer.* 7:880–887. http://dx.doi.org/10.1038/nrc2250

Corzo, C.A., T. Condamine, L. Lu, M.J. Cotter, J.I. Youn, P. Cheng, H.I. Cho, E. Celis, D.G. Quiceno, T. Padhya, et al. 2010. HIF-1α regulates function and differentiation of myeloid-derived suppressor cells in the tumor microenvironment. *J. Exp. Med.* 207:2439–2453. http://dx.doi.org/10.1084/jem.20100587

De Palma, R., I. Marigo, F. Del Galdo, C. De Santo, P. Serafini, S. Cingarlini, T. Tüting, J. Lenz, G. Basso, G. Milan, et al. 2004. Therapeutic effectiveness of recombinant cancer vaccines is associated with a prevalent T-cell receptor alpha usage by melanoma-specific CD8+ T lymphocytes. *Cancer Res.* 64:8068–8076. http://dx.doi.org/10.1158/0008-5472.CAN-04-0067

De Santo, C., P. Serafini, I. Marigo, L. Dolcetti, M. Bolla, P. Del Soldato, C. Melani, C. Guiducci, M.P. Colombo, M. Iezzi, et al. 2005. Nitroaspirin corrects immune dysfunction in tumor-bearing hosts and promotes tumor eradication by cancer vaccination. *Proc. Natl. Acad. Sci. USA.* 102:4185–4190. http://dx.doi.org/10.1073/pnas.0409783102

Doedens, A.L., C. Stockmann, M.P. Rubinstein, D. Liao, N. Zhang, D.G. DeNardo, L.M. Coussens, M. Karin, A.W. Goldrath, and R.S. Johnson. 2010. Macrophage expression of hypoxia-inducible factor-1 alpha suppresses T-cell function and promotes tumor progression. *Cancer Res.* 70:7465–7475. http://dx.doi.org/10.1158/0008-5472.CAN-10-1439

Frederick, M.J., and G.L. Clayman. 2001. Chemokines in cancer. *Expert Rev. Mol. Med.* 3:1–18. http://dx.doi.org/10.1017/S1462399401003301

Fridlender, Z.G., G. Buchlis, V. Kapoor, G. Cheng, J. Sun, S. Singhal, M.C. Crisanti, L.C. Wang, D. Heitjan, L.A. Snyder, and S.M. Albelda. 2010. CCL2 blockade augments cancer immunotherapy. *Cancer Res.* 70:109–118. http://dx.doi.org/10.1158/0008-5472.CAN-09-2326

Gabrilovich, D.I., and S. Nagaraj. 2009. Myeloid-derived suppressor cells as regulators of the immune system. *Nat. Rev. Immunol.* 9:162–174. http://dx.doi.org/10.1038/nri2506

Galon, J., A. Costes, F. Sanchez-Cabo, A. Kirilovsky, B. Mlecnik, C. Lagorce-Pagès, M. Tosolini, M. Camus, A. Berger, P. Wind, et al. 2006. Type, density, and location of immune cells within human colorectal tumors predict clinical outcome. *Science.* 313:1960–1964. http://dx.doi.org/10.1126/science.1129139

Gattinoni, L., D.J. Powell Jr., S.A. Rosenberg, and N.P. Restifo. 2006. Adoptive immunotherapy for cancer: building on success. *Nat. Rev. Immunol.* 6:383–393. http://dx.doi.org/10.1038/nri1842

Griscavage, J.M., A.J. Hobbs, and L.J. Ignarro. 1995. Negative modulation of nitric oxide synthase by nitric oxide and nitroso compounds. *Adv. Pharmacol.* 34:215–234. http://dx.doi.org/10.1016/S1054-3589(08)61088-1

Grohmann, U., and V. Bronte. 2010. Control of immune response by amino acid metabolism. *Immunol. Rev.* 236:243–264. http://dx.doi.org/10.1111/j.1600-065X.2010.00915.x

Hamzah, J., M. Jugold, F. Kiessling, P. Rigby, M. Manzur, H.H. Marti, T. Rabie, S. Kaden, H.J. Gröne, G.J. Hämmerling, et al. 2008. Vascular normalization in Rgs5-deficient tumours promotes immune destruction. *Nature.* 453:410–414. http://dx.doi.org/10.1038/nature06868

Harlin, H., Y. Meng, A.C. Peterson, Y. Zha, M. Tretiakova, C. Slingluff, M. McKee, and T.F. Gajewski. 2009. Chemokine expression in melanoma metastases associated with CD8+ T-cell recruitment. *Cancer Res.* 69:3077–3085. http://dx.doi.org/10.1158/0008-5472.CAN-08-2281

Homey, B., A. Müller, and A. Zlotnik. 2002. Chemokines: agents for the immunotherapy of cancer? *Nat. Rev. Immunol.* 2:175–184. http://dx.doi.org/10.1038/nri748

Hu, H., L. Sun, C. Guo, Q. Liu, Z. Zhou, L. Peng, J. Pan, L. Yu, J. Lou, Z. Yang, et al. 2009. Tumor cell-microenvironment interaction models coupled with clinical validation reveal CCL2 and SNCG as two predictors of colorectal cancer hepatic metastasis. *Clin. Cancer Res.* 15:5485–5493. http://dx.doi.org/10.1158/1078-0432.CCR-08-2491

Huang, B., Z. Lei, J. Zhao, W. Gong, J. Liu, Z. Chen, Y. Liu, D. Li, Y. Yuan, G.M. Zhang, and Z.H. Feng. 2007. CCL2/CCR2 pathway mediates recruitment of myeloid suppressor cells to cancers. *Cancer Lett.* 252:86–92. http://dx.doi.org/10.1016/j.canlet.2006.12.012

Izhak, L., G. Wildbaum, U. Weinberg, Y. Shaked, J. Alami, D. Dumont, B. Friedman, A. Stein, and N. Karin. 2010. Predominant expression of CCL2 at the tumor site of prostate cancer patients directs a selective loss of immunological tolerance to CCL2 that could be amplified in a beneficial manner. *J. Immunol.* 184:1092–1101. http://dx.doi.org/10.4049/jimmunol.0902725

Johnson, L.A., R.A. Morgan, M.E. Dudley, L. Cassard, J.C.Yang, M.S. Hughes, U.S. Kammula, R.E. Royal, R.M. Sherry, J.R. Wunderlich, et al. 2009. Gene therapy with human and mouse T-cell receptors mediates cancer regression and targets normal tissues expressing cognate antigen. *Blood.* 114:535–546. http://dx.doi.org/10.1182/blood-2009-03-211714

June, C.H. 2007. Adoptive T cell therapy for cancer in the clinic. *J. Clin. Invest.* 117:1466–1476. http://dx.doi.org/10.1172/JCI32446

Kaplan-Lefko, P.J., T.M. Chen, M.M. Ittmann, R.J. Barrios, G.E. Ayala, W.J. Huss, L.A. Maddison, B.A. Foster, and N.M. Greenberg. 2003. Pathobiology of autochthonous prostate cancer in a pre-clinical transgenic mouse model. *Prostate.* 55:219–237. http://dx.doi.org/10.1002/pros.10215

Kasic, T., P. Colombo, C. Soldani, C.M. Wang, E. Miranda, M. Roncalli, V. Bronte, and A. Viola. 2011. Modulation of human T-cell functions by reactive nitrogen species. *Eur. J. Immunol.* 41:1843–1849. http://dx.doi.org/10.1002/eji.201040868

Kurata, S., M. Matsumoto, and U. Yamashita. 1996. Concomitant transcriptional activation of nitric oxide synthase and heme oxygenase genes during nitric oxide-mediated macrophage cytostasis. *J. Biochem.* 120:49–52.

Loetscher, P., M. Seitz, I. Clark-Lewis, M. Baggiolini, and B. Moser. 1996. Activation of NK cells by CC chemokines. Chemotaxis, Ca2+ mobilization, and enzyme release. *J. Immunol.* 156:322–327.

Loos, T., A. Mortier, and P. Proost. 2009. Chapter 1. Isolation, identification, and production of posttranslationally modified chemokines. *Methods Enzymol.* 461:3–29. http://dx.doi.org/10.1016/S0076-6879(09)05401-9

Marigo, I., E. Bosio, S. Solito, C. Mesa, A. Fernandez, L. Dolcetti, S. Ugel, N. Sonda, S. Bicciato, E. Falisi, et al. 2010. Tumor-induced tolerance and

immune suppression depend on the C/EBPbeta transcription factor. *Immunity*. 32:790–802. http://dx.doi.org/10.1016/j.immuni.2010.05.010

Mariotto, S., L. Cuzzolin, A. Adami, P. Del Soldato, H. Suzuki, and G. Benoni. 1995. Effect of a new non-steroidal anti-inflammatory drug, nitroflurbiprofen, on the expression of inducible nitric oxide synthase in rat neutrophils. *Br. J. Pharmacol*. 115:225–226.

Melillo, G., T. Musso, A. Sica, L.S. Taylor, G.W. Cox, and L. Varesio. 1995. A hypoxia-responsive element mediates a novel pathway of activation of the inducible nitric oxide synthase promoter. *J. Exp. Med*. 182:1683–1693. http://dx.doi.org/10.1084/jem.182.6.1683

Mennuni, C., S. Ugel, F. Mori, B. Cipriani, M. Iezzi, T. Pannellini, D. Lazzaro, G. Ciliberto, N. La Monica, P. Zanovello, et al. 2008. Preventive vaccination with telomerase controls tumor growth in genetically engineered and carcinogen-induced mouse models of cancer. *Cancer Res*. 68:9865–9874. http://dx.doi.org/10.1158/0008-5472.CAN-08-1603

Monegal, A., D. Ami, C. Martinelli, H. Huang, M. Aliprandi, P. Capasso, C. Francavilla, G. Ossolengo, and A. de Marco. 2009. Immunological applications of single-domain llama recombinant antibodies isolated from a naïve library. *Protein Eng. Des. Sel*. 22:273–280. http://dx.doi.org/10.1093/protein/gzp002

Morgan, R.A., M.E. Dudley, J.R. Wunderlich, M.S. Hughes, J.C. Yang, R.M. Sherry, R.E. Royal, S.L. Topalian, U.S. Kammula, N.P. Restifo, et al. 2006. Cancer regression in patients after transfer of genetically engineered lymphocytes. *Science*. 314:126–129. http://dx.doi.org/10.1126/science.1129003

Mukai, S., J. Kjaergaard, S. Shu, and G.E. Plautz. 1999. Infiltration of tumors by systemically transferred tumor-reactive T lymphocytes is required for antitumor efficacy. *Cancer Res*. 59:5245–5249.

Murphy, P.M. 2001. Chemokines and the molecular basis of cancer metastasis. *N. Engl. J. Med*. 345:833–835. http://dx.doi.org/10.1056/NEJM200109133451113

Muzaffar, S., N. Shukla, G. Angelini, and J.Y. Jeremy. 2004. Nitroaspirins and morpholinosydnonimine but not aspirin inhibit the formation of superoxide and the expression of gp91phox induced by endotoxin and cytokines in pig pulmonary artery vascular smooth muscle cells and endothelial cells. *Circulation*. 110:1140–1147. http://dx.doi.org/10.1161/01.CIR.0000139851.50067.E4

Nagaraj, S., K. Gupta, V. Pisarev, L. Kinarsky, S. Sherman, L. Kang, D.L. Herber, J. Schneck, and D.I. Gabrilovich. 2007. Altered recognition of antigen is a mechanism of CD8+ T cell tolerance in cancer. *Nat. Med*. 13:828–835. http://dx.doi.org/10.1038/nm1609

Nathan, C., and A. Ding. 2010. SnapShot: reactive oxygen intermediates (ROI). *Cell*. 140:951–951: e2. http://dx.doi.org/10.1016/j.cell.2010.03.008

Noda, S., S.A. Aguirre, A. Bitmansour, J.M. Brown, T.E. Sparer, J. Huang, and E.S. Mocarski. 2006. Cytomegalovirus MCK-2 controls mobilization and recruitment of myeloid progenitor cells to facilitate dissemination. *Blood*. 107:30–38. http://dx.doi.org/10.1182/blood-2005-05-1833

Pagès, F., A. Berger, M. Camus, F. Sanchez-Cabo, A. Costes, R. Molidor, B. Mlecnik, A. Kirilovsky, M. Nilsson, D. Damotte, et al. 2005. Effector memory T cells, early metastasis, and survival in colorectal cancer. *N. Engl. J. Med*. 353:2654–2666. http://dx.doi.org/10.1056/NEJMoa051424

Pfeiffer, S., A. Lass, K. Schmidt, and B. Mayer. 2001. Protein tyrosine nitration in cytokine-activated murine macrophages. Involvement of a peroxidase/nitrite pathway rather than peroxynitrite. *J. Biol. Chem*. 276:34051–34058. http://dx.doi.org/10.1074/jbc.M100585200

Pivarcsi, A., A. Müller, A. Hippe, J. Rieker, A. van Lierop, M. Steinhoff, S. Seeliger, R. Kubitza, U. Pippirs, S. Meller, et al. 2007. Tumor immune escape by the loss of homeostatic chemokine expression. *Proc. Natl. Acad. Sci. USA*. 104:19055–19060. http://dx.doi.org/10.1073/pnas.0705673104

Quezada, S.A., K.S. Peggs, M.A. Curran, and J.P. Allison. 2006. CTLA4 blockade and GM-CSF combination immunotherapy alters the intratumor balance of effector and regulatory T cells. *J. Clin. Invest*. 116:1935–1945. http://dx.doi.org/10.1172/JCI27745

Rollins, B.J., and M.E. Sunday. 1991. Suppression of tumor formation in vivo by expression of the JE gene in malignant cells. *Mol. Cell. Biol*. 11:3125–3131.

Rosenberg, S.A., and M.E. Dudley. 2009. Adoptive cell therapy for the treatment of patients with metastatic melanoma. *Curr. Opin. Immunol*. 21:233–240. http://dx.doi.org/10.1016/j.coi.2009.03.002

Rosenberg, S.A., N.P. Restifo, J.C. Yang, R.A. Morgan, and M.E. Dudley. 2008. Adoptive cell transfer: a clinical path to effective cancer immunotherapy. *Nat. Rev. Cancer*. 8:299–308. http://dx.doi.org/10.1038/nrc2355

Rossi, C.A., M. Flaibani, B. Blaauw, M. Pozzobon, E. Figallo, C. Reggiani, L. Vitiello, N. Elvassore, and P. De Coppi. 2011. In vivo tissue engineering of functional skeletal muscle by freshly isolated satellite cells embedded in a photopolymerizable hydrogel. *FASEB J*. 25:2296–2304. http://dx.doi.org/10.1096/fj.10-174755

Sato, E., S.H. Olson, J. Ahn, B. Bundy, H. Nishikawa, F. Qian, A.A. Jungbluth, D. Frosina, S. Gnjatic, C. Ambrosone, et al. 2005. Intraepithelial CD8+ tumor-infiltrating lymphocytes and a high CD8+/regulatory T cell ratio are associated with favorable prognosis in ovarian cancer. *Proc. Natl. Acad. Sci. USA*. 102:18538–18543. http://dx.doi.org/10.1073/pnas.0509182102

Serbina, N.V., T. Jia, T.M. Hohl, and E.G. Pamer. 2008. Monocyte-mediated defense against microbial pathogens. *Annu. Rev. Immunol*. 26:421–452. http://dx.doi.org/10.1146/annurev.immunol.26.021607.090326

Sozzani, S., M. Locati, D. Zhou, M. Rieppi, W. Luini, G. Lamorte, G. Bianchi, N. Polentarutti, P. Allavena, and A. Mantovani. 1995. Receptors, signal transduction, and spectrum of action of monocyte chemotactic protein-1 and related chemokines. *J. Leukoc. Biol*. 57:788–794.

Springer, T.A. 1994. Traffic signals for lymphocyte recirculation and leukocyte emigration: the multistep paradigm. *Cell*. 76:301–314. http://dx.doi.org/10.1016/0092-8674(94)90337-9

Suzuki, M., M. Tabuchi, M. Ikeda, and T. Tomita. 2002. Concurrent formation of peroxynitrite with the expression of inducible nitric oxide synthase in the brain during middle cerebral artery occlusion and reperfusion in rats. *Brain Res*. 951:113–120. http://dx.doi.org/10.1016/S0006-8993(02)03145-1

Szabó, C., H. Ischiropoulos, and R. Radi. 2007. Peroxynitrite: biochemistry, pathophysiology and development of therapeutics. *Nat. Rev. Drug Discov*. 6:662–680. http://dx.doi.org/10.1038/nrd2222

Ugel, S., E. Scarselli, M. Iezzi, C. Mennuni, T. Pannellini, F. Calvaruso, B. Cipriani, R. De Palma, L. Ricci-Vitiani, E. Peranzoni, et al. 2010. Autoimmune B-cell lymphopenia after successful adoptive therapy with telomerase-specific T lymphocytes. *Blood*. 115:1374–1384. http://dx.doi.org/10.1182/blood-2009-07-233270

Viola, A., and V. Bronte. 2007. Metabolic mechanisms of cancer-induced inhibition of immune responses. *Semin. Cancer Biol*. 17:309–316. http://dx.doi.org/10.1016/j.semcancer.2007.06.005

Viola, A., and A.D. Luster. 2008. Chemokines and their receptors: drug targets in immunity and inflammation. *Annu. Rev. Pharmacol. Toxicol*. 48:171–197. http://dx.doi.org/10.1146/annurev.pharmtox.48.121806.154841

Weishaupt, C., K.N. Munoz, E. Buzney, T.S. Kupper, and R.C. Fuhlbrigge. 2007. T-cell distribution and adhesion receptor expression in metastatic melanoma. *Clin. Cancer Res*. 13:2549–2556. http://dx.doi.org/10.1158/1078-0432.CCR-06-2450

Xia, Y., and J.L. Zweier. 1997. Superoxide and peroxynitrite generation from inducible nitric oxide synthase in macrophages. *Proc. Natl. Acad. Sci. USA*. 94:6954–6958. http://dx.doi.org/10.1073/pnas.94.13.6954

Xia, Y., L.J. Roman, B.S. Masters, and J.L. Zweier. 1998. Inducible nitric-oxide synthase generates superoxide from the reductase domain. *J. Biol. Chem*. 273:22635–22639. http://dx.doi.org/10.1074/jbc.273.35.22635

Zhang, B., Y. Zhang, N.A. Bowerman, A. Schietinger, Y.X. Fu, D.M. Kranz, D.A. Rowley, and H. Schreiber. 2008. Equilibrium between host and cancer caused by effector T cells killing tumor stroma. *Cancer Res*. 68:1563–1571. http://dx.doi.org/10.1158/0008-5472.CAN-07-5324